Journal of the Korean Physical Society, Vol. 42, No. 1, January 2003, pp. 153∼157

Optical Analysis of Self-Assembled InAs/GaAs Quantum-Dot Heterostructures Based on Far-Infrared Absorption and Near-Infrared Emission

S. K. Kang, S. J. Lee, M. D. Kim and S. K. Noh*

Quantum Dot Technology Laboratory, Korea Research Institute of Standards and Science, Daejeon 305-600

J. W. Choe

Department of Electrical Engineering and Computer Science, Kyunghee University, Suwon 449-701

(Received 15 October 2002)

We report some electronic characteristics of a couple of self-assembled InAs/GaAs quantum-dot (QD) heterostructures with sizes of 1.8 and 2.0 monolayers (MLs) fabricated by using the molecular beam epitaxial technique via the Stranski-Krastanow growth mode. Optical analysis of the far-infrared absorption spectra and the near-infrared photoluminescence (PL) emission spectra taken at room temperature has been made in order to determine the energy positions of the sublevels in the QD *ensemble*. The absorption peak energies (wavelengths) are identified as 90 meV (13.8 μm) and 110 meV (11.3 μm), and the PL emission peak energies are 1.202 eV and 1.169 eV for 1.8-ML and 2.0-ML QD samples at room temperature, respectively. On the basis of the absorption and the emission spectra, we propose schematic energy-band diagrams for 1.8-ML and 2.0-ML InAs-QD/GaAs heterostructures.

PACS numbers: 78.55.Cr; 78.66.Fd; 85.30.Vw
Keywords: Quantum dot, Far infrared absorption spectrum, Photoluminescence, Self-assembling technique, Molecular beam epitaxy

I. INTRODUCTION

Semiconductor quantum dots (QDs) and related devices have been receiving much attention as unique zero-dimensional systems in nano-scale physics and device engineering. To date, in the compound semiconductor region utilized by self-assembling techniques [1], remarkable progress in the areas of QD-based laser diodes (QDLD) [2–5] and infrared photodetectors (QDIP) [6–10] has been made by using various layer structures to realize high-frequency direct-modulation or normal-incidence operation at room temperature, thus overcoming the limitation of quantum-well-based devices. Since the QD heterostructure, which controls the absorption and the emission processes of photons, plays a critical role in these devices as an active layer, more understanding not only of QD-based devices but also of the physical and the electronic characteristics of QDs themselves is required.

A number of theoretical and experimental studies have been done on InAs-based QDs in the last a few years [11–26]. Based on the experimental evidence, Grundmann *et al.* [16] proposed an electronic level scheme of InAs pyramidal QDs from numerical calculation of the single particle problem for electrons and holes with a Coulomb correlation. Jiang and Singh [11] reported some theoretical results on the electronic spectra for InAs-QD/GaAs heterostructures by using the effective mass approximation for the conduction band and a four-band $\mathbf{k}\cdot\mathbf{p}$ model for the valence band. Sauvage *et al.* [17] presented experimental results on the energy positions of electron and hole sublevels in InAs QDs by using mid-infrared absorption and photoluminescence (PL) at low temperature (200 K), and Ghosh *et al.* [18] used deep-level transient spectroscopy (DLTS) measurements to present a schematic profile showing the sublevel energy position and the conduction band offset. Recently, a schematic conduction band diagram was given by Kim *et al.* [19] on the basis of the intraband photocurrent from biased QDIP structures. In addition, Bras *et al.* [20] reported evidence for the existence of polaron states associated with strong electron-phonon coupling from the temperature dependence of the intrasublevel absorption in InAs QDs obtained through a theoretical analysis of the thermionic emission of carriers. Although many papers have been published on QD heterostructures investigated by using a variety of measurement techniques [11–26], the energy band scheme illustrating the transition

*E-mail: sknoh@kriss.re.kr

behavior in the QD *ensemble* is still rather ambiguous and scattered.

In this paper, we report some electronic results from the normal-incidence far-infrared (FIR) absorption spectra and the near-infrared (NIR) PL emission spectra taken at room temperature (300 K) in a couple of Si-doped InAs QDs with different sizes. We will propose a schematic band diagram for the InAs-QD/GaAs heterostructure. The diagram was constructed by combining the measured values of the absorption energy and the emission energy.

II. EXPERIMENTAL

A couple of Si-doped InAs/GaAs heterostructures with an active layer of five-period multi-layered InAs-QDs (MQDs) were grown by using a molecular beam epitaxy (MBE) system (RIBER 32P). All the devices were grown under the same conditions by using the self-assembling QD technique of the Stranski-Krastanow (S-K) growth mode and basically had the same layer profile, except for the equivalent thickness of InAs for size control of the QD *ensemble*. The growth was conducted at temperatures of 560/520 °C for the GaAs buffer/cap layer and 480 °C for the active layer of the InAs-QD/GaAs-barrier. The growth rates of InAs and GaAs were 1.4 nm/min and 12.4 nm/min, respectively, and the V/III beam-equivalent pressure (BEP) was approximately 25. The equivalent thicknesses of the single InAs-QD layer of each structure were 1.8 and 2.0 monolayers (MLs), and the growth of the InAs-QD/GaAs-barrier layer was repeated for five periods. The QD formation was initiated on a 0.3-μm GaAs buffer layer, and the barrier layer was covered by 10-nm-thick undoped GaAs between sequential QD layers. The Si-doping of 1×10^{17} cm^{-3} was carried out during a period of 30 s just after the initial stage of QD formation. The details of the epitaxial growth and the basic properties have been reported elsewhere [25,26]. The FIR absorption measurements were performed by using a commercial Fourier-transformed infrared (FTIR) spectrophotometer (Equinox 55) at room temperature (300 K), and the NIR PL spectra were taken from a typical visible-to-NIR spectrometer system with a closed-cycle He refrigerator (10 K) and an Ar-ion laser (514.5 nm).

III. RESULTS AND DISCUSSION

Figure 1 demonstrates a couple of surface images (1 μm $\times$ 1 μm) obtained by using an atomic force microscope (AFM) for uncapped single-layered QD (SQD) structures with thicknesses of (a) 1.8 MLs and (b) 2.0 MLs, which were equivalent to samples used in this study. The QD densities evaluated from the surface profiles were

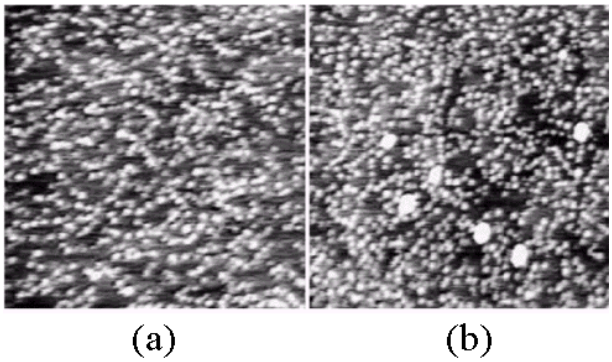

Fig. 1. AFM surface images (1 μm $\times$ 1 μm) for uncapped SQD structures with thicknesses of (a) 1.8 ML and (b) 2.0 ML equivalent to the samples used in this study. The dot densities are (a) $\sim 8 \times 10^{10}$ cm^{-2} and (b) $\sim 1 \times 10^{11}$ cm^{-2} with an overall size fluctuation of (a) 10 % and (b) 18 %.

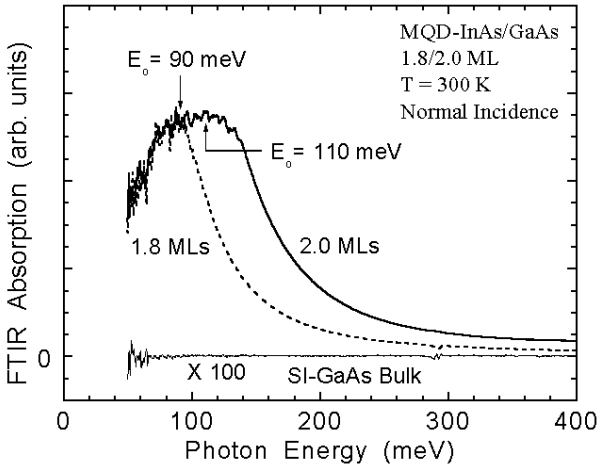

Fig. 2. Three normal-incidence FTIR absorption curves measured at 300 K for two MQD structures and a SI-GaAs bulk. While the SI-GaAs bulk as a control sample gives no absorption signal, absorption peaks are clearly observed near 90 meV (13.8 μm) and 110 meV (11.3 μm) for the 1.8-ML (dotted line) and the 2.0-ML (solid line) MQD structures, respectively.

$\sim 8 \times 10^{10}$ cm^{-2} and $\sim 1 \times 10^{11}$ cm^{-2}, and the average dot dimensions [long baseline $\times$ short baseline $\times$ height] were approximately [29 $\times$ 19 $\times$ 1.4] nm and [31 $\times$ 22 $\times$ 1.5] nm with size fluctuations of 10 % and 18 % for 1.8 MLs and 2.0 MLs, respectively. While both the average size of the QDs and their density simultaneously increased a little with increasing equivalent thickness, there was a considerable decrease in the overall size uniformity, as shown in the AFM images.

The room-temperature absorption measurements were made on both structures at normal incidence by using the FTIR spectrometer. Figure 2 shows three FIR absorption curves, two for MQD structures and one for semi-insulating (SI) GaAs as functions of the incident photon energy. While the SI-GaAs bulk, as a control

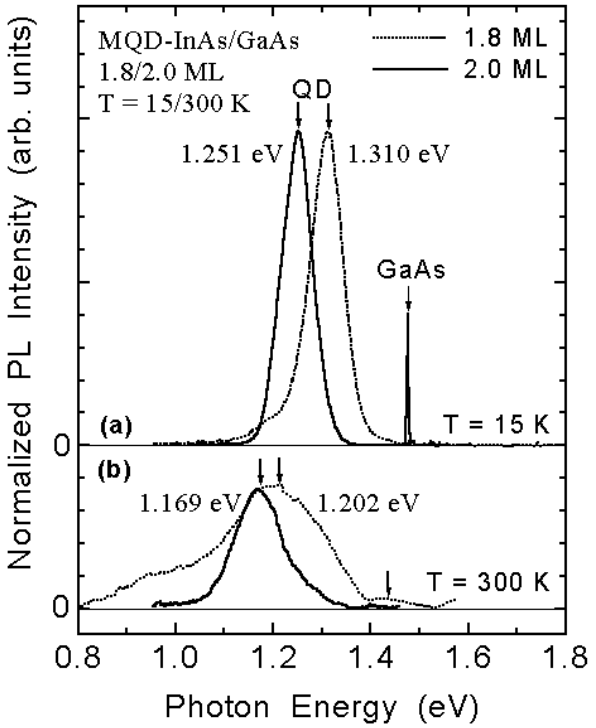

Fig. 3. NIR PL spectra measured at (a) 15 K and (b) 300 K for two MQD structures. The curves are normalized to the peak intensity. Because of the smaller size of the QD *ensemble*, the PL peak of the 1.8-ML sample (dotted lines) resides at a higher energy position than that of the 2.0-ML sample (solid lines).

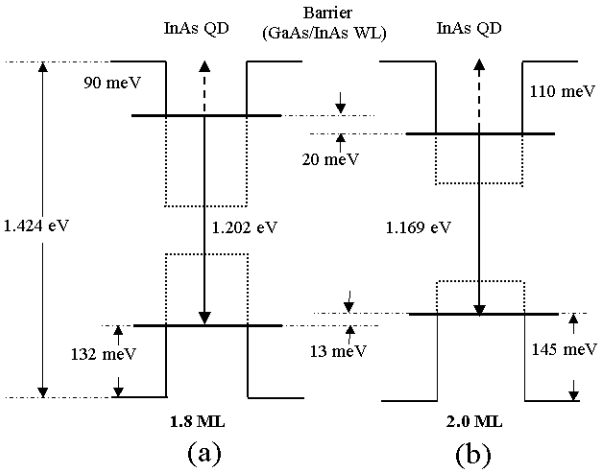

Fig. 4. Schematic energy-band diagrams for (a) the 1.8-ML and (b) the 2.0-ML InAs-QD/GaAs heterostructures presented in this study. The energy positions of the sublevels from the conduction/valence band of the barrier due to the GaAs barrier and the InAs wetting layers are estimated as 90/132 meV and 110/145 meV for the 1.8-ML and 2.0-ML structures, respectively. The dotted lines stand for non-defined energy levels in the QDs.

sample, gives no absorption signal within the noise level, the absorption peaks are clearly observed near 90 meV (13.8 μm) and 110 meV (11.3 μm) in energy (wavelength) with an reading error of $\pm$10 meV (approximately $\pm$1.0 μm) for the 1.8-ML (dotted line) and 2.0-ML (solid line) structures, respectively. Since the peak energy can adequately correspond to the transition energy of bound-to-continuum states, 90/110 meV can be taken as the energy separation from the conduction sublevel of an InAs QD to the continuum barrier states of GaAs and/or the InAs wetting layer (WL) [17]. Thus, if we get the interband transition energy, it would be possible to make the energy band profile of QD heterostructures by using the sublevel-to-continuum transition energy extracted from the FIR absorption spectra.

Figure 3 presents PL spectra obtained at (a) 15 K and (b) 300 K for two QD structures. The details of the spectra can be attributed to the interband transition between the conduction and the valence sublevels. The peak energies at 15/300 K are 1.310/1.202 eV and 1.251/1.169 eV for the 1.8-ML and the 2.0-ML samples, respectively. The energy difference between the PL peaks for 15 K and 300 K resulted from the temperature dependence of the bandgap energy, and the higher PL energy of the 1.8-ML sample, compared to that of the 2.0-ML one, is attributed to the smaller size of the QD *ensemble*, as previously mentioned. Using the PL emission energy and the absorption energy obtained at 300 K, we have proposed a pair of energy-band schematics for the InAs-QD/GaAs heterostructures used in this study, as illustrated in Fig. 4. The dotted lines in Fig. 4 stand for non-defined energy levels in QDs, and a value of 1.424 eV has been adopted for the bandgap energy of the GaAs bulk at 300 K. Here, we have assumed that the QD *ensemble* has a single level both in the conduction and the valence bands [17–19].

We have identified that the energy separations from the QD sublevel to the continuum barrier states of the conduction/valence band in an InAs-QD/GaAs heterostructure are 90/132 meV and 110/145 meV for the 1.8-ML and the 2.0-ML QD samples fabricated in this study, respectively. While the theoretical values reported for the sublevel energy are very scattered in a broad range of 100-183 meV for the conduction sublevel and 20-253 meV for the valence one in InAs QDs [11, 16], the experimental results reported so far are quite consistent with the theoretical values. Sauvage *et al.* [17] have reported a conduction sublevel separated by 190 meV from the conduction band of GaAs barrier and a valence sublevel spacing of 115 meV by using the photo-induced absorption experiment, and Kim *et al.* [21] have presented a range of 180-250 meV for the bound-to-continuum transition on the basis of photocurrent analysis. Using the activation energy from the DLTS signal, Ghosh *et al.* [19] proposed a QD sublevel separated by 120 meV from the GaAs conduction band and a band offset of (341$\pm$30) meV. Even though direct comparison

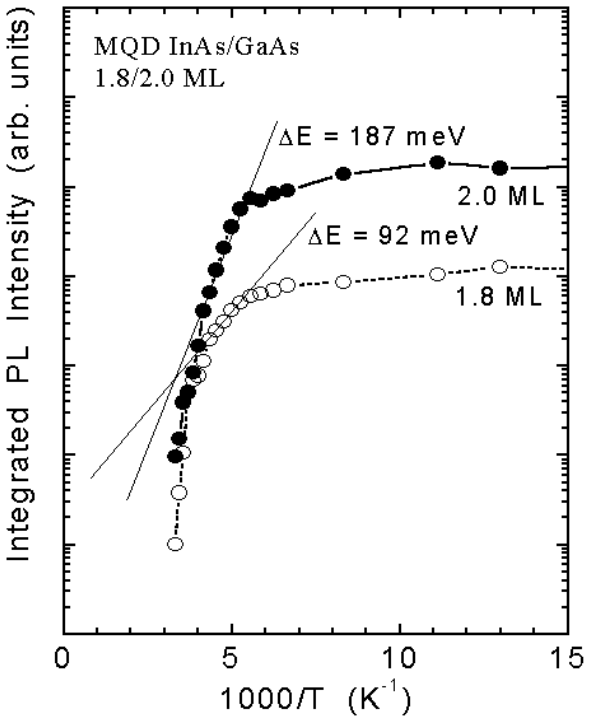

Fig. 5. Plots for the integrated PL intensity versus the inverse temperature. Linear fits to the curves reveal the activation energies of 92 meV and 187 meV for the 1.8-ML (open circles) and the 2.0-ML (solid circles) structures, respectively.

among the reported values may have little importance because of the diversity in QD sizes and shapes, it would be very meaningful for the values of 90/132 meV and 110/145 meV presented in this study to be comparable to, or in agreement with, the reported values considering the reasonable experimental errors. The schematic band diagram in Fig. 4 does not show an exact band profile, but it gives the transition scheme in the QD *ensemble*, as well as some useful references on relative positions of the sublevels in bands or between structures.

Finally, we discuss the activation energy determined from the temperature dependence of the integrated PL intensity. The activation energy is known to follow the functional form exp[-ΔE/kT], where ΔE is the activation energy of electrons or holes and kT the thermal energy. Figure 5 shows plots of the integrated PL intensity versus the inverse temperature and an experimental fit of exp[-ΔE/kT] to the linear section for each plot. The activation energies (ΔE) estimated by using least-squares fit are approximately 92 meV and 187 meV within the fitting error range of ±10 meV for the 1.8-ML (open circles) and the 2.0-ML (solid circles) QD structures, respectively. It is interesting that ΔE≅92 meV for the 1.8-ML QD sample is close to 90 meV for the conduction sublevel, but the activation energy of 187 meV is very different from 110 meV for the conduction sublevel for the 2.0-ML sample. Although it is very difficult to discuss the agreement or the discrepancy at the present stage, we understand that the large difference in the activation energy may result from a mixed behavior due to both electrons and holes being generated by photoexcitation.

IV. SUMMARY

In summary, we have reported some electronic parameters which were obtained from the normal-incidence FIR absorption spectra and the NIR PL spectra taken at room temperature from a couple of Si-doped InAs-QD/GaAs heterostructures with equivalent thicknesses of 1.8 MLs and 2.0 MLs. The transition energies of the bound-to-continuum states in the conduction band of 90 meV and 110 meV were taken from the absorption peaks, and the interband transition energies of 1.202 eV and 1.169 eV were determined from the PL emission peaks (300 K). Assuming the existence of a single sublevel in each band, we proposed a pair of schematic energy-band diagrams for InAs/GaAs QD heterostructures with different QD sizes. The diagrams showed the transition scheme and the relative positions of the sublevels in bands or between structures.

ACKNOWLEDGMENTS

This work was mainly carried out at the National Research Laboratory on Quantum Dot Technology (Contract No. M1-0104-00-0127) in the Korea Research Institute of Standards and Science (KRISS) designated by the Ministry of Science and Technology (MOST), and was supported in part by the Korea Science and Engineering Foundation (KOSEF) (Contract No. R01-2000-00034). One of the authors (SKN) acknowledges the partial support provided by the Science Research Center of Quantum Functional Devices.

REFERENCES

[1] D. Bimberg, M. Grundmann and N. N. Ledentsov, *Quantum Dot Heterostructures* (Wiley, New York, 1999).
[2] M. Grundmann, Physica E **5**, 167 (2000).
[3] G. Park, O. B. Shchenkin, S. Csutak, D. L. Huffaken and D. G. Deppe, Appl. Phys. Lett. **75**, 3267 (1999).
[4] J. Takebayashi, M. Nishioka and Y. Arakawa, Appl. Phys. Lett. **78**, 3469 (2001).
[5] G. Walter, T. Chung and N. Holonyak, Jr., Appl. Phys. Lett. **80**, 1126 (2002).
[6] E. Towe and D. Pan, IEEE J. Select. Topics Quant. Electron. **6**, 408 (2000).
[7] A. D. Stiff, S. Krishna, P. Bhattacharya and S. W. Kennerly, IEEE J. Quant. Electron. **37**, 1412 (2001).

[8] S.-W. Lee, K. Hirakawa and Y. Shimada, Appl. Phys. Lett. **75**, 1428 (1999).
[9] M. D. Kim, A. G. Choo, S. S. Ko, D. H. Park and S. C. Hong, J. Korean Phys. Soc. **39**, 32 (2001).
[10] A. D. Stiff-Roberts, S. Chakrabarti, S. Pradhan, B. Kochman and P. Bhattacharya, Appl. Phys. Lett. **80**, 3265 (2002).
[11] H. Jiang and J. Singh, IEEE J. Quantum Electron. **34**, 1188 (1998).
[12] J. Phillips, J. Appl. Phys. **91**, 4590 (2002).
[13] S.-K. Eah, W. Jhe and Y. Arakawa, Appl. Phys. Lett. **80**, 2779 (2002).
[14] U. H. Lee, J. K. Yim, D. Lee, H. G. Lee, S. K. Noh, J. Y. Leem and H. J. Lee, J. Korean Phys. Soc. **37**, 593 (2000).
[15] J. S. Kim, P. W. Yu, J. Y. Leem, J. I. Lee, S. K. Noh, J. S. Kim, S. M. Kim and J. S. Son, Appl. Phys. Lett. **78**, 3247 (2001).
[16] M. Grundmann, O. Stier and D. Bimberg, Phys. Rev. B **52**, 11969 (1995).
[17] S. Sauvage, P. Boucaud, F. H. Julien, J.-M. Gerard and J.-Y. Marzin, J. Appl. Phys. **82**, 3396 (1997).
[18] S. Ghosh, B. Kochman, J. Singh and P. Bhattacharya, Appl. Phys. Lett. **76**, 2571 (2000).
[19] E.-T. Kim, Z. Chen and A. Madhukar, Appl. Phys. Lett. **79**, 3341 (2001).
[20] F. Bras, P. Boucaud, S. Sauvage, G. Fishman and J.-M. Gerard, Appl. Phys. Lett. **80**, 4620 (2002).
[21] R. Heitz, I. Mukhametzhanov, O. Stier, A. Madhukar and D. Bimberg, Phys. Rev. Lett. **83**, 4654 (1999).
[22] N. Horiguchi, T. Futatsugi, Y. Nakata, N. Yokoyama, T. Mankad and P.M. Petroff, Jpn. J. Appl. Phys. **38**, 2559 (1999).
[23] D. Pan, E. Towe and S. Kennerly, Appl. Phys. Lett. **73**, 1937 (1998).
[24] Q. D. Zhung, J. M. Li, H. X. Li, Y. P. Zeng, L. Pan, Y. H. Chen, M. Y. Kong and L. Y. Lin, Appl. Phys. Lett. **73**, 3706 (1998).
[25] J. S. Kim, P. W. Yu, J. Y. Leem, J. I. Lee, S. K. Noh, J. S. Kim, G. H. Kim, S. K. Kang, S. I. Bahn, S. G. Kim, Y. D. Jang, U. H. Lee, J. S. Yim and D. H. Lee, J. Cryst. Growth **234**, 105 (2002).
[26] J. S. Kim, P. W. Yu, J. Y. Leem, S. K. Noh, J. I. Lee, J. S. Kim, S. M. Kim, G. H. Kim, S. K. Kang, S. G. Kim and J. S. Son, J. Korean Phys. Soc. **39**, S246 (2001).